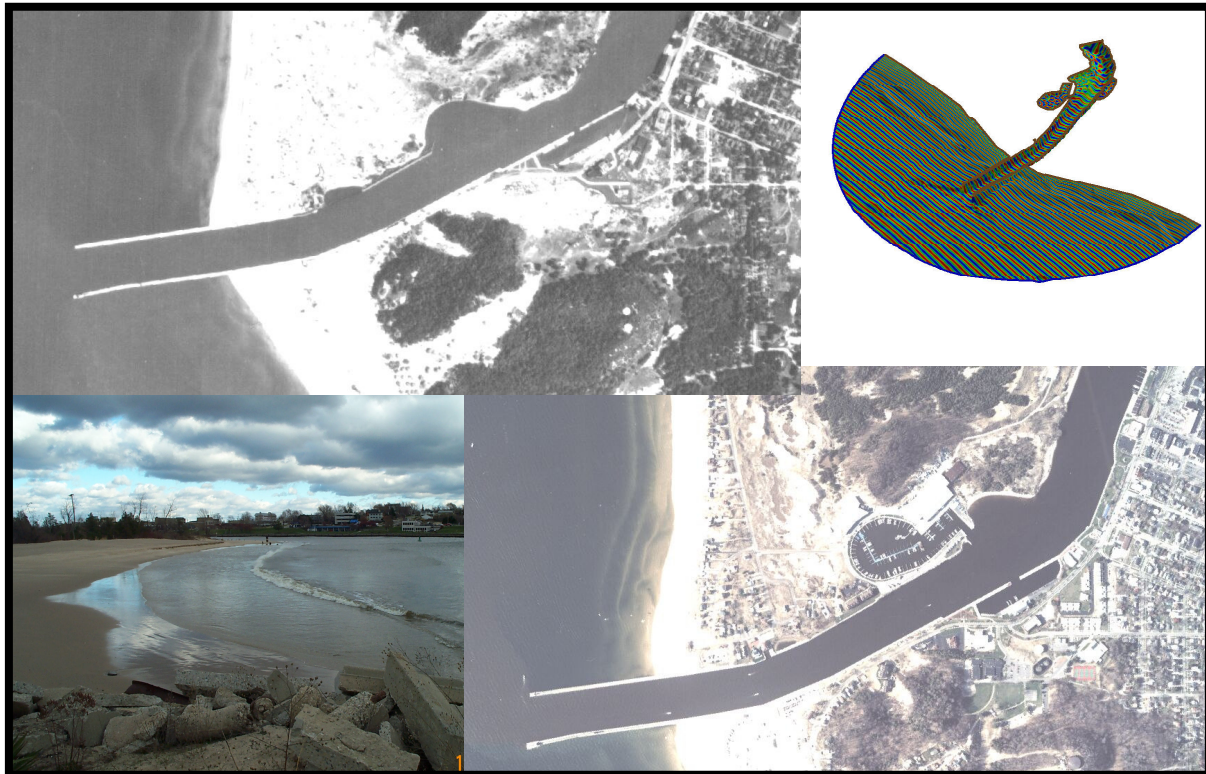**SECTION 111 REPORT**

Wave Erosion Analysis

April 2004

Grand Haven NOWS Project
Ottawa County, Michigan

U.S. Army Corps of Engineers
Detroit District
Great Lakes Hydraulics and Hydrology Office

Table of Contents

FIGURES

TABLES

APPENDICES

Appendix A: CGWAVE Model Results

Appendix B: Wave Amplitudes (m) Arcs 1-5

Appendix C: Wave Energy Arcs A,B, C

1.0 Introduction

1.1 Purpose of Study

The purpose of this study is to determine the effect Federal navigation structures at Grand Haven Harbor, Michigan, have on erosion at Kitchel-Lindquist Dunes (study site) within the harbor. Various wave heights and directions will be analyzed and modeled to determine increased wave energy at the site in question. Furthermore, historical aerial photography will be analyzed to confirm the nature of the erosion at the site as well as to document any changes in the harbor over its lifetime.

1.2 Authority and Acknowledgments

The USACE is authorized to investigate mitigation of shore damage attributable to Federal Navigation under Section 111 of the Rivers and Harbors Act of 1968. The Coastal and Hydraulic Laboratory (CHL) of the U.S. Army Corps of Engineers (USACE) performed detailed coastal hydraulic modeling for this study. The USACE Detroit District analyzed modeling results and aerial photography. This work was provided at the request of the Northwest Ottawa Water System (NOWS).

2.0 Scope of Study

Grand Haven Harbor is located about 100 miles northeasterly of Chicago, Illinois in Ottawa County Michigan on Lake Michigan (Figure 1). The harbor is the natural outlet of the Grand River, which has a drainage basin of 5,572 square mile (Section 111, DPR, 1976).

The study site is located approximately 5000 ft eastward from the harbor mouth on the north side of the navigation channel (figure 2). It is an actively eroding area adjacent to a marina.

2.1 Harbor History
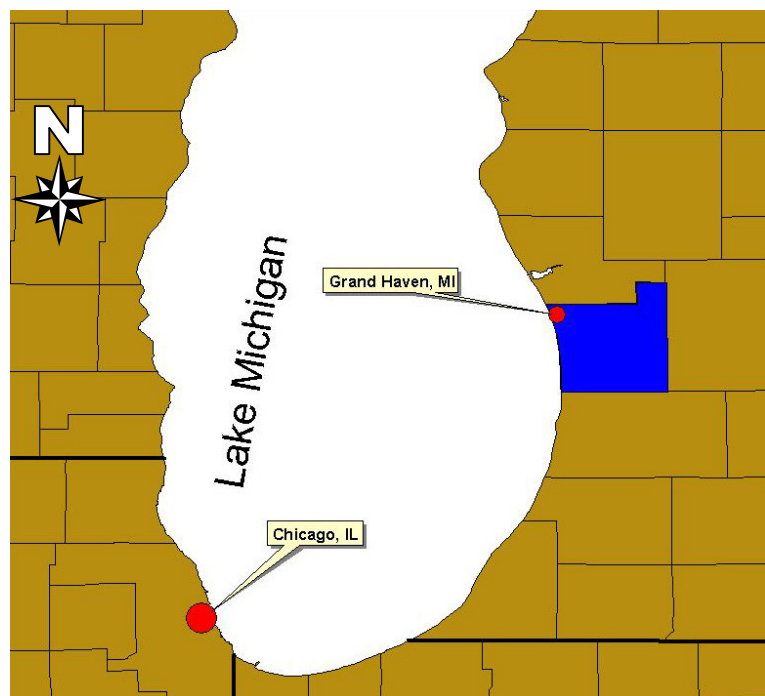
Figure 1: Location Map

Construction of protective structures at the harbor entrance began as early as 1857 when a revetment was placed along the south bank near the mouth of the Grand River. The River and Harbors Act of June 23, 1866 authorized the first Federal work. The Federal project provided two parallel, close piling piers, extending lakeward from the river mouth. Construction on the south pier was incrementally done between 1867 and 1894. The north pier was constructed in sections between 1875 and 1894. The final work in 1894 brought the piers to their present lengths.

Figure 2: Location of Study Site within Navigation Channel

The Federal channel is 300 feet wide and 23 feet deep up to 1000 feet inside the pier ends. After the first 1000 feet, the channel becomes 21 feet deep for approximately 2-1/2 miles to the Grand Trunk Railway Bridge at Ferrysburg (Section 111 DPR, 1976).

Since 1894, the basic pier configuration has remained unchanged. However, there have been numerous projects in the last 110 years that have altered the geometry and functionality of the inner harbor area. The first of these projects was the installation of a marina (Figure 3) on the north side of the channel. Regulatory permit information (Grand Haven Area Office (GHAO), 2004) indicates the marina was completed by 1953. Comparison of the 1938 and 1955 aerial photographs in figure 3 shows the geometric changes to the federal harbor between these two temporal periods. This represents the most significant changes to the internal layout of the harbor during its recent history (1938 to present).
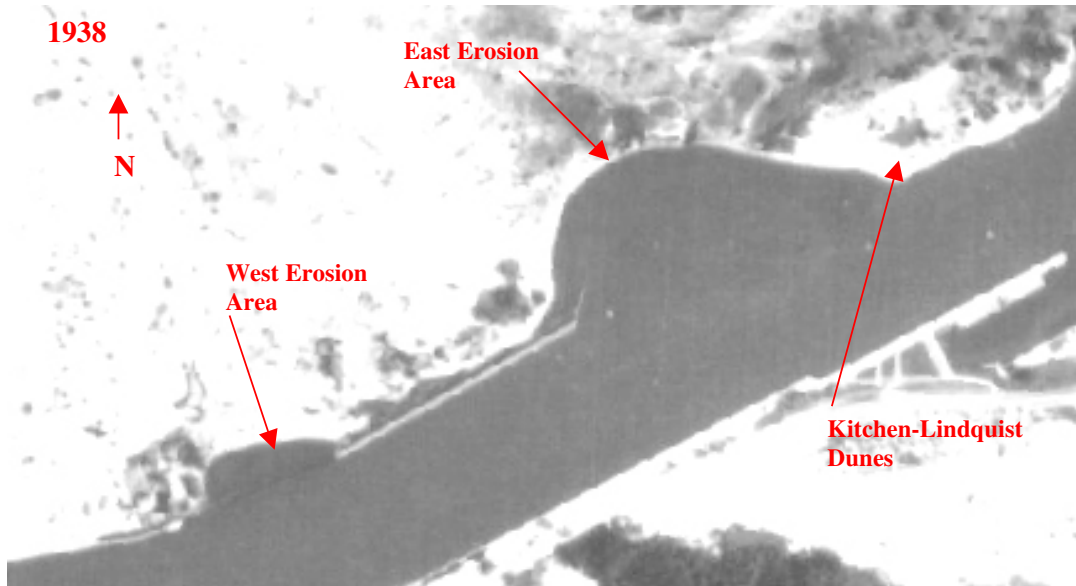
A) Study Site and Adjacent Areas in 1938
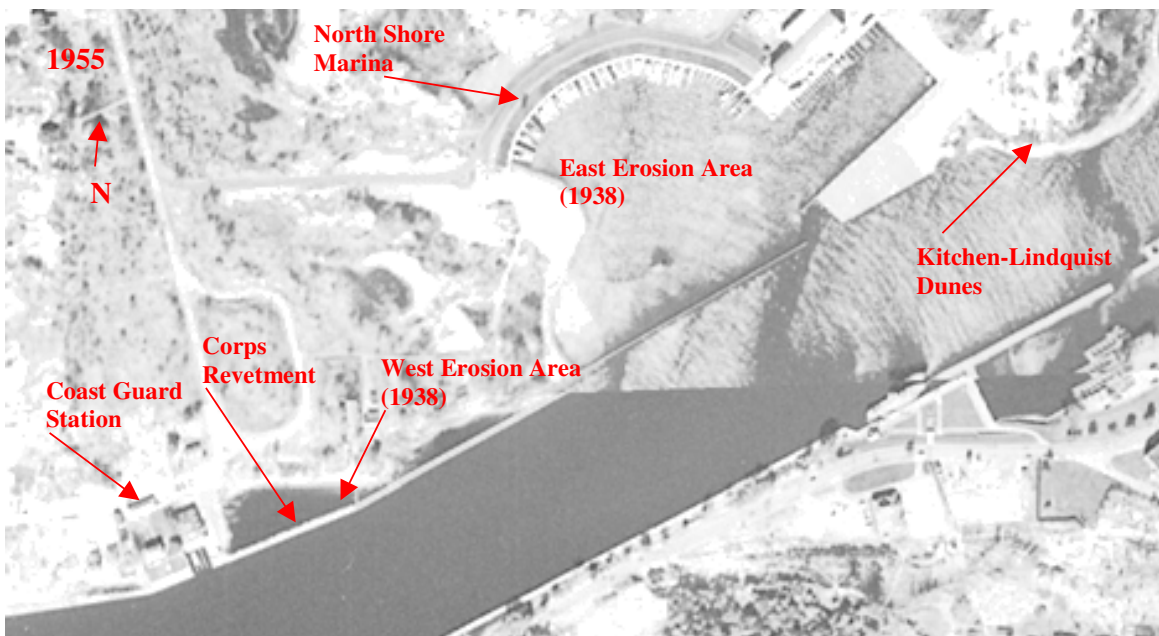
B) Study Site and Adjacent Areas in 1955

Figure 3:Inner Harbor Area in 1938 and 1955

Harbor repair projects have also taken place at Grand Haven at various times from 1952 to present. Repairs have included work to the substructure, superstructure, and installation of Steel Sheet Pile (SSP). Table 1 and figure 4 detail the numerous repair projects that have been accomplished.

Two important items need to be pointed out concerning repair projects over the harbor's history. First, numerous SSP installation projects have been accomplished to incrementally encase of approximately 9060 feet of stone cribbing between 1952 and 1984. Figure 5 illustrates the areas along the channel that have been encased with SSP and in what time period. Secondly, in 1955, the revetment along the north side of the channel was extended across a natural erosion area (Figure 3). The installation of this SSP eliminated an innate wave energy absorption area increasing the chances of waves propagating further up the channel.

TABLE 1A

Data found in the Project Map Book for Grand Haven Harbor

TABLE 1B

(See note below)

North Side

Section	Length (feet)	Substructure	Superstructure	Repaired	SSP Installation
A1	55	1984	1921	1953	***
A	48	1887,89,91,94	1921	1953 - 55	***
A2	108	1894	1921	1952	***
A	600	1887,89,91,94	1921	1953 - 55	***
B	605	1875,77,78,79	1922	1957 - 58	1958
C	9	1873-74,1932	1932	1957	***
C1	191	1873-74,1932	1932	1957	1984
D	406	1873-74	1932		1984
E	677	1873-74,1911	1938	1981	1981
F	726	1917-18	1917-18	1963	1963
G	150	1918	1918		*

South Side

Section	Length (feet)	Substructure	Superstructure	Repaired	SSP Installation
H	119	1893-94	1921-22	1957	1957
H1	652	1883-85,87,91-93	1921-22	1954	***
I	348	1892-94	1919-20	1951,52,57	1957
J	78	1868-69,1919-20	1919-20	1957,59-60	1960
J1	31	1868-69,1919-20	1919-20	1957,59-60	1960
K	287	1867-68,1916-17	1916-17	1959-60	1960
L	315	1857-58,64,1908-09	1935	1972	1972
M	452	1857-58,1910-11	1935	1972	1972
N	353	1857-58,1916-1918	1916-18	1963	1963
O	324	1857-58,1916-1918	1916-18	1963	1963
P	1164	1872-75,1910-11	1936-37		1984
Q	26	1910-11	1933	1972	1972
R1	73	1910-11	1933-34	1972	1972
R2-R3	260	1857-58,1910-11	1935	1972	1972
R4-R5	394	1857-58,1910-11	1935	1972	1972
S	477	1910-11	1930	1962	1962
T	136	1910-11,14	1930	1962	1962

Notes:

1. Table 1B represents dates of SSP installation verified by the Record of Construction or As-built Drawings.

2. Regulatory permit information, found in GHAO, indicates the North Shore Marina was in by 1953. No other information is available to know its exact construction date.

3. * The Project Map indicates Section G does not contain SSP. It states it is not maintained and is covered with sand. Structure Inspections performed in 2003 verify this information, other than there are four pairs of SSP visible. A educated guess is they were installed when the SSP was installed for Section F(1963).

4. *** Denotes where the date for SSP installation should be the same date as shown in the "Repaired" column. These dates fluctuate slighty between the dates found on Project Maps and As-built drawings. It is safe to say the SSP was driven within three years of the "Repaired" column date.

Table 1: Grand Haven Harbor repairs (1952 to present)

In 2002, NOWS requested the USACE to initiate a Section 14, Emergency Shore Protection project within the study site to protect a 20" water transmission line exposed thru erosion processes. In May 2003 sediment dredged from the outer harbor was placed at the study site to temporarily protect the transmission line from erosion forces until a more permanent solution could be found.
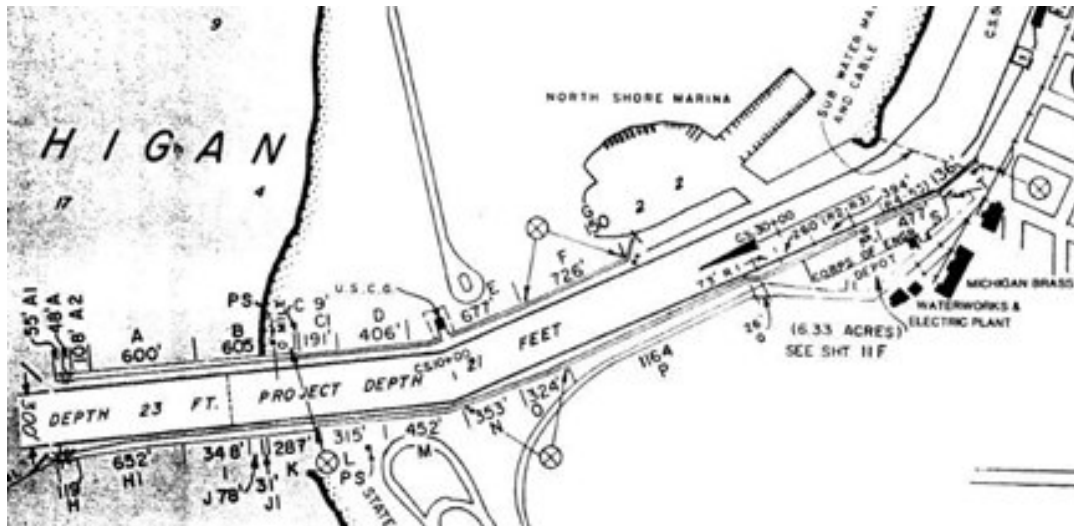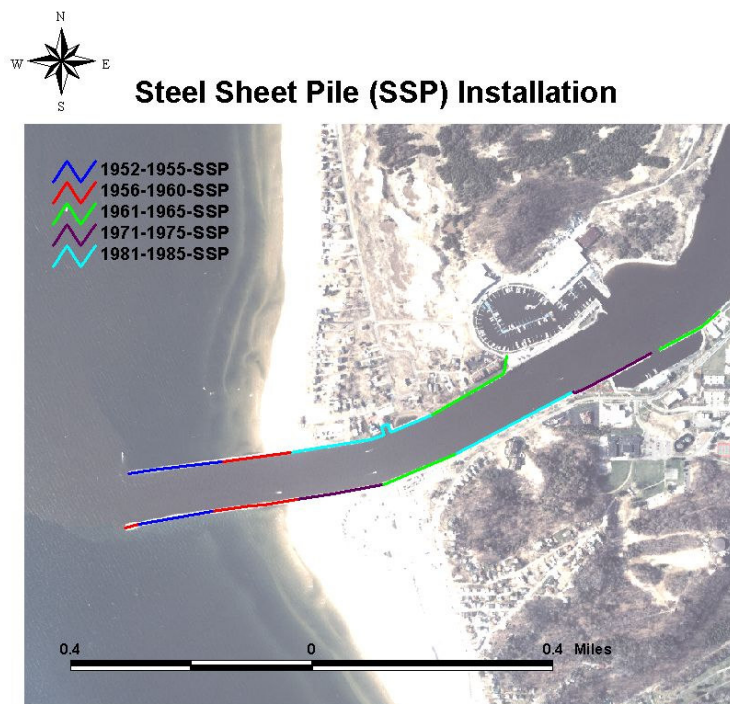

Figure 4: Grand Haven Harbor repairs (1952 to present)

Figure 5: SSP Installation

3.0 Data Sources

This section describes the spatial and temporal data used in this study. It includes a description of the raw data and how it was organized for use in the modeling efforts.

3.1 Wave Data

The nearest Wave Information Study (WIS) station to Grand Haven is Station 52. As part of the WIS program conducted by USACE, a 2D Hindcast was completed for Lake Michigan from 1956 to 1987 (Hubertz et al., 1991) and then extended to 1997. The 2D method has three broad steps: 1) model grid development, 2) create wind fields for the entire model domain from available wind data, and 3) predict wave conditions at each grid point. There were several limitations with the Lake Michigan WIS Hindcast. First the grid is very coarse (10 mile^2 resolution). Secondly, bathymetry was omitted from the study and deep-water conditions were assumed. Thirdly, ice impacts were not considered. And lastly, only a small number of wind stations were used for a large domain area (Lake Michigan).

In a report prepared by Baird and Associates (Baird, 1999), substantial changes in the directionality and total wave energy were noted between the WIS data generated for the periods 1956 to 1987 and 1988 to 1997. A 1D parametric wind-wave hindcast was performed by Baird and Associates for the USACE's Lake Michigan Potential Damages Study (LMPDS, 2000) for a period from 1956 to 1998. In 2003, the hindcast was extended to cover the time period from 1999 to 2002. The hindcast location is approximately 10 km offshore of Allegan County and corresponds to the location of WIS Station 55, which is approximately 40 miles south of Grand Haven.

Recognizing that wave hincasting has undergone substantial advances in the last two decades, and the new hindcast at WIS Station 55 covered a larger and more recent temporal period, it was desirable to use the Baird hindcast at station 55 over the outdated WIS hindcast at station 52. It needed to be determined whether the information at station 55 could be translated to station 52. Figure 6 is a comparison of WIS data from station 55 to station 52. Good correlation was seen between wave directions at the two stations. Furthermore, an evaluation of wave height frequency at the two locations shows good correspondence (figure 7).

Wave Direction Frequency

■ Station 55 (Baird) ■ Station 52 (WIS)
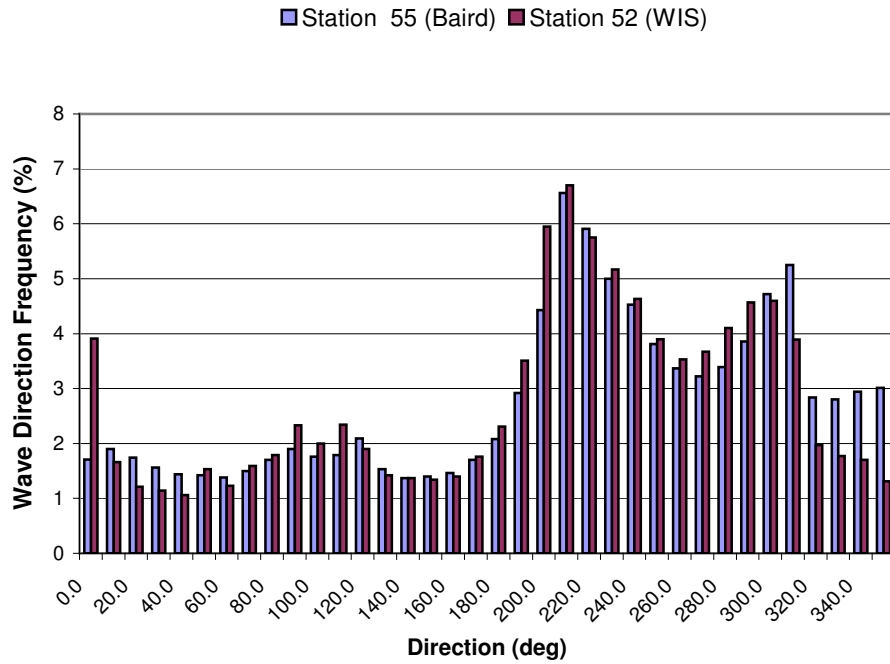
Figure 6: WIS Data Comparison to Baird 1-D Hindcast

Wave Height vs. Frequency

■ Station 55 (Baird) ■ Station 52 (WIS)
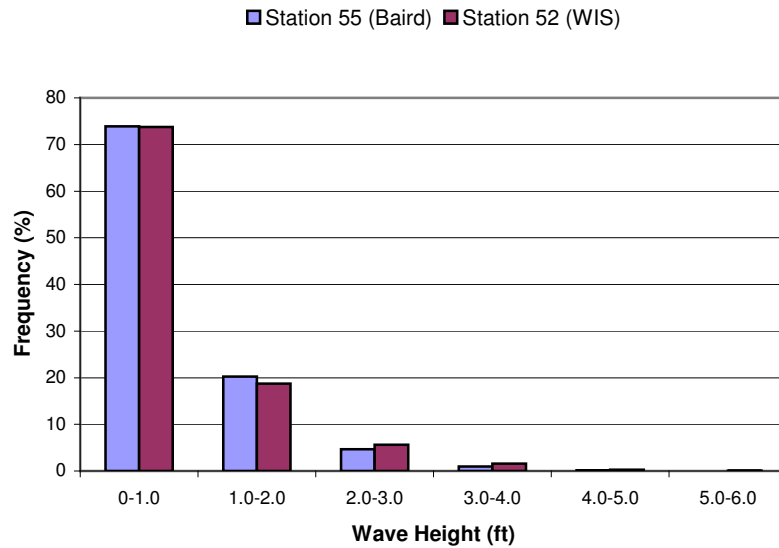
Figure 7: Wave Height Frequency Comparison

Based on the data comparison described above, it was evident that the Baird hindcast covering the temporal period of 1949 to 2002 at station 55 would adequately represent the wave climate at Grand Haven. The wave rose presented in figure 8 represents the total wave climate expected at Grand Haven. Waves seem to mostly be from the northwest and southwest quadrants.
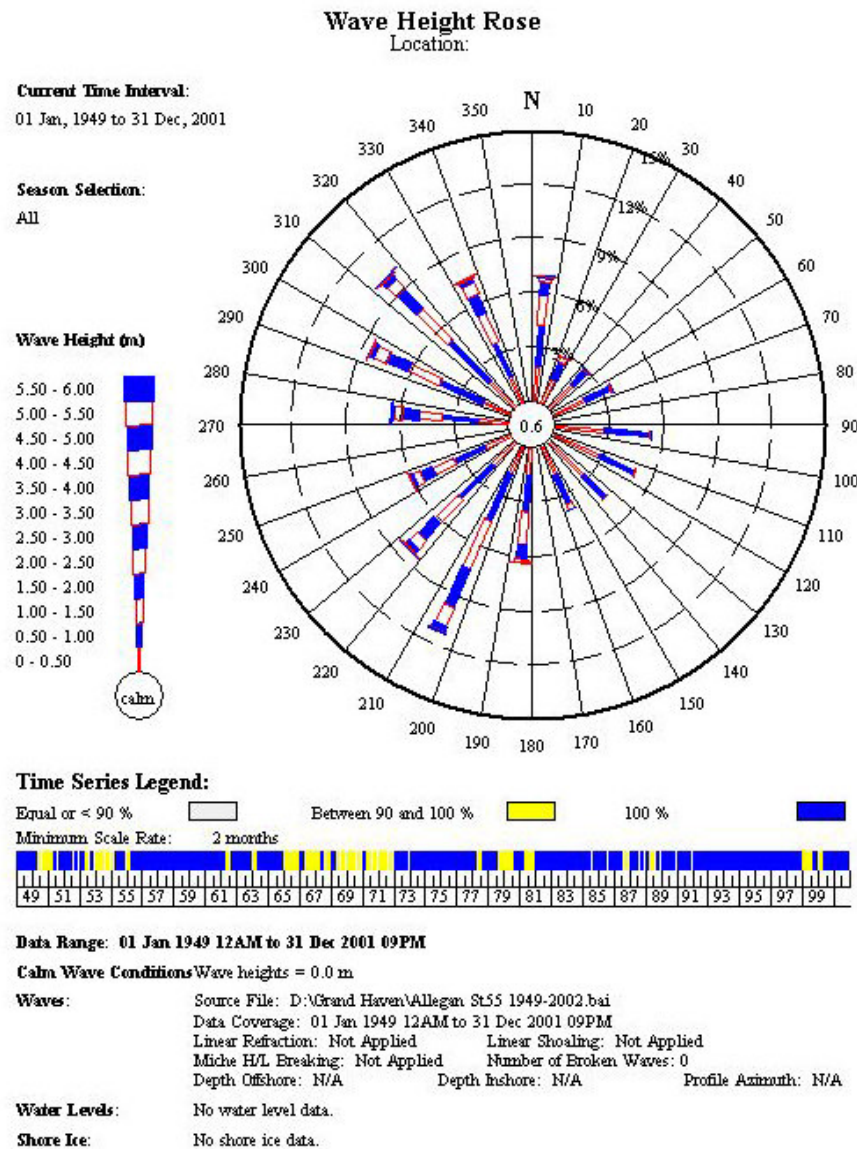
Figure 8: Wave Height Rose

3.2 Bathymetry

The bathymetry used in this study was produced from two sources. Bathymetry for the open coast was produced from a 2001 SHOALS survey. Bathymetry for the inner harbor area was created from Condition Surveys performed by GHAO in May of 2003. The two data sets were merged without any problem and used in the grid development for numerical modeling efforts (figure 9).
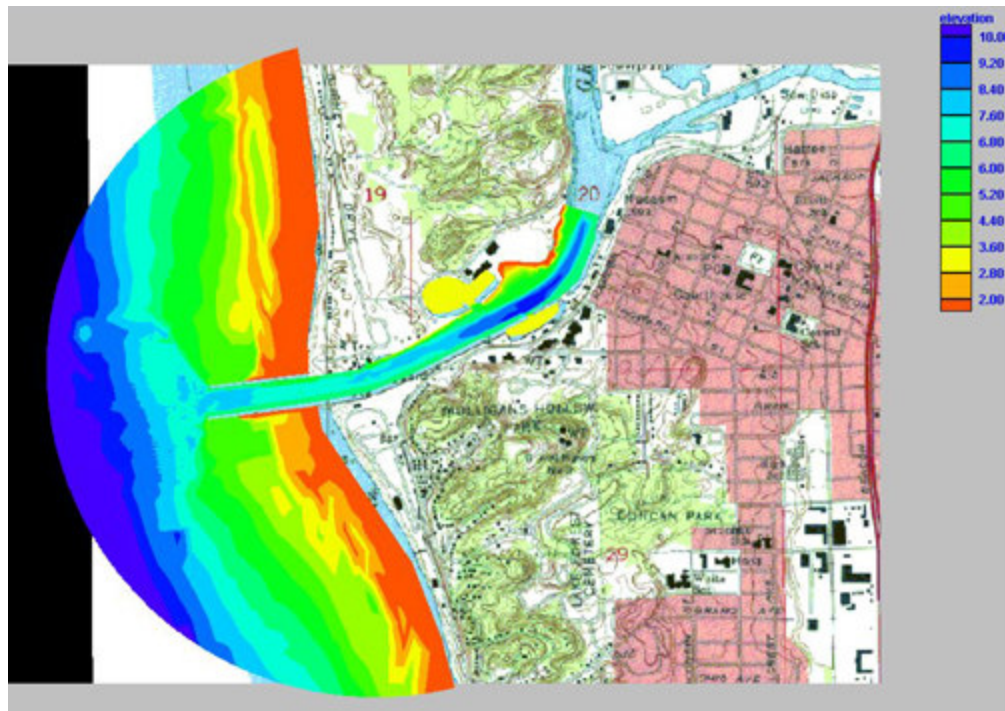
Figure 9: Bathymetry (shoals survey 2001 & GHAO condition survey: May 2003)

3.3 Aerial Photography

Aerial photography was used in this analysis to provide historical information on the harbor, recession rate information on the erosion zone, and boundary condition information for numerical modeling. Aerial photography for Grand Haven harbor was available for the years 1938, 1955, 1968, and 1978. Digital Orthoquads (DOQs) were available for the year 1997 and Digital Orthophotos (DOPs) were available for 2003, both projected to Universal Transverse Mercator (UTM) coordinate system, Zone 16 north, meters. The aerial photography was georeferenced to the same coordinate sytem using the DOQs and DOPs.

4.0 Coastal Modeling

One coastal model was applied to quantify the wave climate in Grand Haven Harbor. CGWAVE is a state-of-the-art wave-agitation model used to describe the wave climates in enclosed areas such as bays and harbors. CGWAVE was utilized to model two scenarios: 1) Grand Haven Harbor as it was in 1938 (Scenario 1)and 2) Grand Haven Harbor in its present configuration (2003) (Scenario 2).

4.1 CGWAVE

Wave climate plays a very important role in all coastal projects. However, in most cases, little wave data are available for engineering construction and planning. Field observation and physical modeling of waves are extremely difficult, costly, and time-consuming. Buoys are far away from the project site, and remote-sensing instruments do not systematically provide wave data at the desired resolution in the near shore region. Since no data-recording instrument can anticipate future "sea" states, the desired "sea"-state information may be obtained and plans evaluated with reliable mathematical modeling techniques.

It is essential to have reliable information on wave conditions for many coastal engineering problems. The most important wave conditions for design and assessment in project studies in the area of interest include the wave heights, wave periods and the dominant wave propagation directions. Typically, these wave parameters are obtained from a wave transformation model that transfers the wave data collected at some remote deep-water site to the location of the project in the near shore. As waves move from deeper waters to approach the shore, these fundamental wave parameters will change as the wave speed changes and wave energy is redistributed along wave crests due to the depth variation between the transfer sites and the presence of islands, background currents, coastal defense structures, and irregularities of the enclosing shore boundaries and other geological features. Waves undergo the severest change inside the surf zone where wave breaking occurs and in the regions where reflected waves from coastline and structural boundaries interact with the incident waves.

Until recently, the linear wave ray theory was used for wave transformation by tracing rays from deep water to the project site near shore. The effects on wave propagation of the wave height and direction along the wave crest are ignored in the ray theory since this theory assumes that wave energy propagates only along a ray and thus, energy flux is conserved between two adjacent rays. As a consequence of this assumption, ray theory breaks down when wave ray crossings and caustics occur because the physics of diffraction are totally ignored in the numerical ray models.

Starting in the early 1980s, coastal designers and researchers have recognized the importance of the combined effects of refraction and diffraction and begun to develop improved theories and associated numerical models. There are indeed several wave theories available that could adequately describe the combined refraction and diffraction of waves from deep water to shallow water (Demirbilek and Webster 1992 and 1998). One of these is the mild-slope equation (MSE). This is a depth-averaged, elliptic type partial differential equation which ignores the evanscent modes (locally emanated waves) and assumes that the rate of change of depth and current within a wavelength is small, hence the 'mild-slope' acronym.

Numerous MSE-based numerical models have been developed for predicting the wave forces on offshore structure and studying wave fields around the offshore islands. Numerical, laboratory and field tests of the MSE models have shown that the MSE can provide accurate solutions to problems where the bottom slope is up to 1:3. From a practical standpoint, the computational requirements for solving the MSE are much larger than those for ray tracing. The reasons for

this are because the MSE is a two-dimensional equation and has to be solved as a boundary-value problem with appropriate boundary conditions. The entire domain of interest must be discretized and solved simultaneously and the element size has to be small enough that there are about 10 to 15 nodes within each wavelength. These requirements place severe demands on computer resources when applying MSE models to large coastal domains. The modeling domain at Grand Haven contained approximately 771,000 and 282,000 nodal points for the 1938 and 2003 scenarios, respectively.

A difficult problem in prediction of waves near shore is to determine where approximately the wave breaking (and breaker line) occurs when waves are inside the sure zone. In numerical models presently used, location is not known a priori, and is usually selected with an ad hoc criteria based on the ratio of wave height to local water depth. Bottom friction and dissipation from the surrounding land boundaries (i.e. entrance losses at the mouth of a harbor) may also be empirically incorporated into MSE models. A simplified version of the MSE is known as the 'parabolic approximation' (PA), which usually reduces the excessive computational demands of MSE model at the expense of further assumptions and simplifications which may render the numerical predictions inaccurate and inappropriate for many coastal and ocean engineering problems (Panchang et al. 1998).

The only purpose of adapting the PA is to convert the MSE to a set of simpler equations that describe a wave propagating in a prescribed direction while still taking both refraction and diffraction in the lateral direction into account. The greatest advantage of PA is its numerical efficiency, it can be solved rather easily by numerical means and thus could be used for predicting wave transformation over a relatively large coastal region. When reflection is of major interest, as it is in harbors, the MSE should be used since the PA ignores reflection. One must also be reminded that the PA that the length scale of the wave amplitude variation in the direction of wave propagation (x direction) is much longer than that in the transverse direction (y direction). The PA is derived on the assumption that percentage changes of depth within a typical wavelength are small compared to the wave slope. For details about PA models, see Booji (1981), Liu (1993), Kirby (1983), Liu and Tsay (1984), and Kirby and Dalrymple (1984). The PA has been verified extensively by laboratory studies and field application (Berkhoff et al. 1982), Liu and Tsay (1984), Kirby and Dalrymple (1984), Vincent and Briggs (1989), (Demirbilek 1994, Demirbilek et al. 1996a and 1996b), and Panching et al. (1998).

The mild-slope wave equation (also known as the "combined refraction-diffraction" equation), first suggested by Eckart (1952) and later re-derived by Berkhoff (1972, 1976) and others, is now well accepted as the method for estimating coastal wave conditions. It can be used to model a wide spectrum of waves, since it passes, in the limit, to the deep and shallow water equations. Although the equation was developed in the mid-seventies, computational difficulties precluded the development of a model for the complete mild-slope equation (except for very small domains). Typically, coastal wave propagation problems involve the modeling of very large domains. For example, consider the case of 12-second waves of 15 m depth. The wavelength L is about 136 m; an 8 km domain is about $3600L^2$ in size. The difficulties associated with solving such large problems spawned the development of several simplified models (e.g. the "parabolic approximation" models (Dalrymple et al. 1984; Kirby, 1986, RCPWAVE model (Ebersole, 1985), EVP model (Panchang et al 1988), etc.). However, these simplified models compromised

the physics of the mild-slope equation: they model only one- or two-way propagation with weak lateral scattering. Such models are hence applicable only to rectangular water domains for a very limited range of wave directions and frequencies. Most realistic coastal domains with arbitrary wave scattering cannot be modeled with these simplified models.

CGWAVE was developed at the University of Maine under a contract for the U.S. Army Corps of Engineers, Waterways Experiment Station (Demirbilek, 1998). CGWAVE is a general purpose, state-of-the-art wave prediction model. It is applicable to estimation of wave fields in harbors, open coastal regions, coastal inlets, around islands, and around fixed or floating structure. While CGWAVE simulates the combined effects of wave refraction-diffraction included in the basic mild-slope equation, it also includes the effects of wave dissipation by friction, breaking, nonlinear amplitude dispersion, and harbor entrance losses. CGWAVE is a finite-element model that is interfaced to the SMS model (Jones & Richards, 1992) for graphics and efficient implementation (pre-processing and post-processing). The classical super-element method as well as a new parabolic approximation method developed recently (Xu, Panchang and Demirbilek 1996), are used to treat the open boundary condition. An iterative suggested procedure (conjugated gradient method) introduced by Panchang et al (1991) and modification suggested by Li (1994) are used to solve the discretized equations, this enabling the modeler to deal with large domain problems.

4.1.1 Basic Equations (CGWAVE)

The solution of the two-dimensional elliptic mild-slope wave equation is a well-accepted method for modeling surface gravity waves in coastal areas (e.g. Chen & Houston, 1987; Chen, 1990; Xu & Panchang, 1993; Mei, 1983; Berkhoff, 1976; Kostense et al. 1986; Tsay and Liu, 1983). This equation may be written as:

$$\nabla \cdot \left(C C_g \nabla \hat{\eta} \right) + \frac{c_g}{C} \sigma^2 \hat{\eta} = 0 \qquad (6)$$

Where

$\hat{\eta}(x, y)$ =   complete surface elevation function, from which the wave height can be estimated

σ =   wave frequency under consideration (in radian/second)

$C(x, y)$ =   phase velocity $= \sigma/k$

$C_g(x, y)$ =   group velocity $= \partial\sigma/\partial k = nC$ with

$$n = \frac{1}{2}\left(1 + \frac{2kd}{\sinh 2kd} \right) \qquad (7)$$

$k(x, y)$ =   wave number $(=2\pi/L)$, related to the local depth $d(x,y)$

through the linear dispersion relation:

$$\sigma^2 = gk \tanh(kd) \tag{8}$$

Equation 7 simulated wave refraction, diffraction, and reflection (i.e. the general wave scattering problem) in coastal domains of arbitrary shape. However, various other mechanisms also influence the behavior of waves in a coastal area. The mild-slope equation can be modified as follows to include the effects of frictional dissipation (Dalrymple et al. 1984; Liu and Tsay 1985) and wave breaking (Dally et al. 1985; De Girolamo et al. 1988):

$$\nabla \cdot \left(CC_g \nabla \hat{\eta}\right) + \left(\frac{C_g}{C}\sigma^2 + i\sigma w + iC_g \sigma \gamma\right)\hat{\eta} = 0 \tag{9}$$

where w is a friction factor and γ is a wave breaking parameter. Following Dalrymple et al. (1984), we have used the following form of the damping factor in CGWAVE:

$$w = \left(\frac{2n\sigma}{k}\right)\left[\frac{2f_r}{3\pi}\frac{ak^2}{(2kd + \sinh 2kd)\sinh kd}\right] \tag{10}$$

where a (= H/2) is the wave amplitude and f_r is a friction coefficient to be provided by the user. The coefficient f_r depends on the Reynolds number and the bottom roughness and may be obtained from Madsen (1976) and Dalrymple et al. (1984). Typically, values for f_r are in the same range as for Manning's dissipation coefficient 'n'. Specifying f_r as a function of (x,y) allows the modeler to assign larger values for elements near harbor entrances to simulate entrance loss. For the wave breaking parameter γ, we use the following formulation (Dally et al. 1985, Demirbilek 1994, Demirbilek et al. 1996b):

$$\gamma = \frac{\chi}{d}\left(1 - \frac{\Gamma^2 d^2}{4a^2}\right) \tag{11}$$

where χ is a constant (a value of 0.15 is used in CGWAVE following Dally et al (1985)) and Γ is an empirical constant (a value of 0.4 is used in CGWAVE).

In addition to the above mechanisms, nonlinear waves may be simulated in the MSE. This is accomplished by incorporating amplitude-dependent wave dispersion, which has been shown to be important in certain situations (Kirby and Dalrymple 1986). The nonlinear dispersion relation used in place of Equation 8 is

$$\sigma^2 = gk\left[1 + (ka)^2 F_1 \tanh^5 kd\right] \tanh\{kd + kaF_2\} \tag{12}$$

where

$$F_1 = \frac{\cosh(4kd) - 2\tanh^2(kd)}{8\sinh^4(kd)}$$

$$F_2 = \left(\frac{kd}{\sinh(kd)}\right)^4$$

(13)

Harbor Application.

The finite-element formulation given above is for open-sea offshore problems. In the case of harbor problems, the formulation is analogous. The only difference arises from the treatment of the open boundary condition. The classical treatment of these problems assumes that the coastlines outside the model domain are straight, collinear, and fully reflective. The exterior wave field written as $\hat{\eta}_{ext} = \hat{\eta}_I + \hat{\eta}_R + \hat{\eta}_S$, where $\hat{\eta}_I, \hat{\eta}_R$, and $\hat{\eta}_S$ represent the incident, the reflected, and the scattered wave fields, respectively. Based on the assumptions, we define (Demirbilek and Gaston 1985)

$$\begin{aligned}
\hat{\eta}_0 &= \hat{\eta}_I + \hat{\eta}_R \\
&= Ae^{ikr\cos(\theta - \theta_I)} + Ae^{ikr\cos(\theta - \theta_I)} \\
&= 2A\sum_{n=0}^{\infty} \varepsilon_n i^n J_n(kr)\cos n\theta_I \cos n\theta
\end{aligned}$$

(14)

where A is the incident wave amplitude and θ_I is the incident wave angle with respect to the exterior coastlines. The scattered wave potential $\hat{\eta}_S$ in the exterior region must take the following form in order to comply with the exterior coastline boundary conditions:

$$\hat{\eta}_S = \sum_{n=0}^{\infty} H_n(kr)\alpha_n \cos n\theta$$

(15)

as shown in Xu, Panshang and Demirbilek (1995). The finite-element formulation of harbor problems can now readily be found in a manner similar to the open-sea problems described above, by replacing $\hat{\eta}_I$ and $\hat{\eta}_S$ and performing the boundary integration for I_4 though I_6 from 0 to π.

4.1.2 Generation of Finite-Element Network

CGWAVE requires a two-dimensional (2D) triangle grid network for its finite-element calculations. Although several grid generation packages are available, they are not suitable for elliptic coastal wave models for which the size of the elements must be related to the wave length (which varies with local water depth) for proper resolution. A semicircular open boundary has to be created for special open boundary treatment, and reflection coefficients, which may vary from one part of the coastal boundary to another, are also required as input data for the model. To deal with these special problems, CGWAVE has been interfaced with the

grid-generator associated with the SMS (Surface water Modeling Systems) flow modeling package. The Engineering Computer Graphics Laboratory is developing this state-of-the-art package for the US Army Corps of Engineers at Brigham Young University.

SMS contains a set of 2D hydrodynamic models and a general-purpose grid generation and visualization package. SMS includes an efficient finite-element grid-generator. However, this grid-generator was originally designed for other types of hydrodynamic models. Three utility programs that help interface CGWAVE with the SMS grid-generator have been developed for use outside SMS, prior to the full integration of CGWAVE into SMS. Given a coarse rectangular array of bathymetric data, these programs generate a wavelength-dependent triangular nodal network (based on the user-specific resolution, i.e. the number of points per wave length), automatically construct the semi-circular open boundary, assign reflection coefficients along the coastal boundaries, eliminate unwanted land points, etc. The resulting grid and boundary data from SMS are then filtered by another utility program for use by the wave model. The output from the wave model can be processed and then plotted by using SMS. This makes model implementation very efficient and allows the user to view a graphic representation of the solution.

4.2 CGWAVE Modeling Inputs for Grand Haven

4.2.1   Wave Input

As discussed in section 3.1, a Baird hindcast was utilized to provide wave data at the open water boundary of the modeling domain (figure 10). Due to the size of the modeling domain and associated time to run CGWAVE, certain wave directions were omitted from the study.
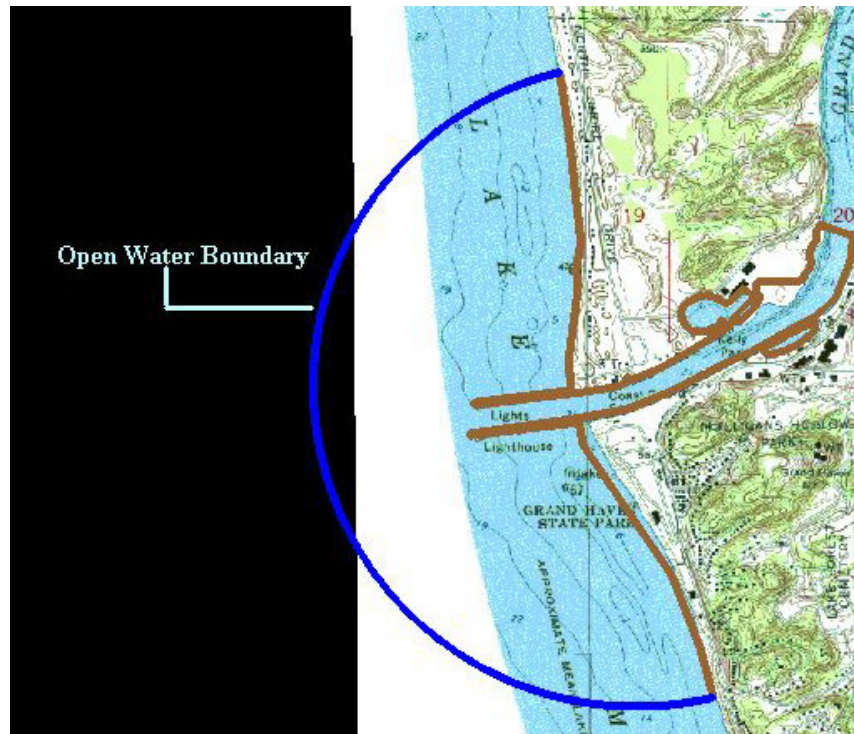
Figure 10: Open Water Boundary

Based on engineering judgment, wave directions ranging from 45° counter-clockwise to 45° clockwise from the centerline of the harbor mouth were selected. Limited wave energy would be expected to propagate down the channel from waves outside of this range due to processes such as refraction, diffraction, and shoaling. The waves within this limit were further reduced to 5 zones (figure 11) for modeling purposes.
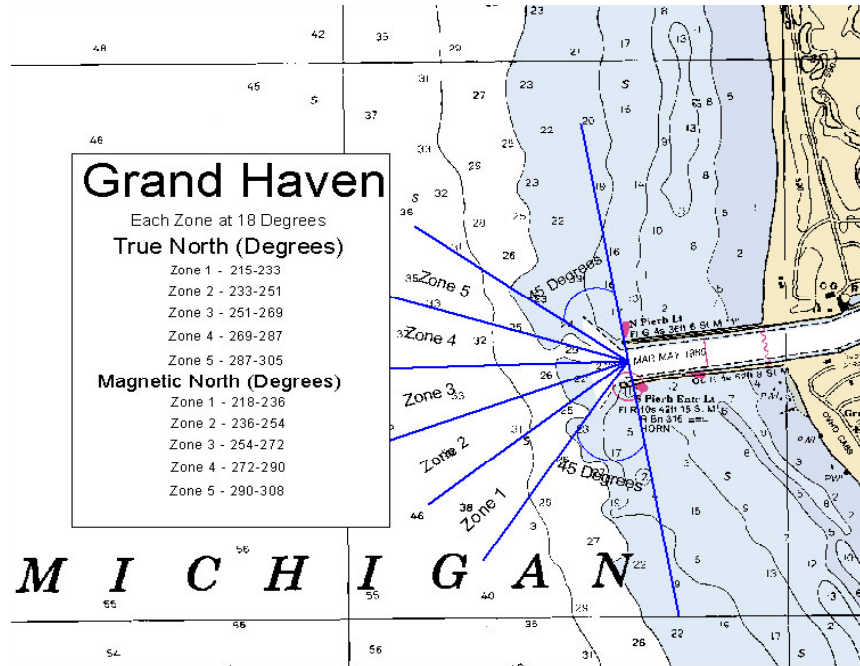
Figure 11: Wave Limit Zones

Waves from all five zones of influence were used to determine the design wave heights to be used in the model. The histogram in figure 12 shows the number of waves that existed for each wave height within the zone limits. Wave heights ranged from 0.2 m (calm) to 4.0 m. The average of the highest 1/3, 1/5, 1/10, 1/20, and 1/50 of the waves in the histogram were chosen to represent the wave climate the harbor has been exposed to in the past for this modeling effort. Table 2 shows the wave heights and periods used for each wave condition used in the model.

Condition	Wave	Height (m)	Period (s)
WC 1	$H_{(1/3)}$	1.97	7
WC 2	$H_{(1/5)}$	2.25	8
WC 3	$H_{(1/10)}$	2.56	8
WC 4	$H_{(1/20)}$	2.82	8
WC 5	$H_{(1/50)}$	3.13	9

Table 2: Wave Heights and Periods

Figure 12: Wave Height Histogram

4.2.2 Grid Development Based on Bathymetric Input

As discussed in section 3.2, survey data was obtained from two sources to create bathymetric input for the CGWAVE model. Bathymetric data was r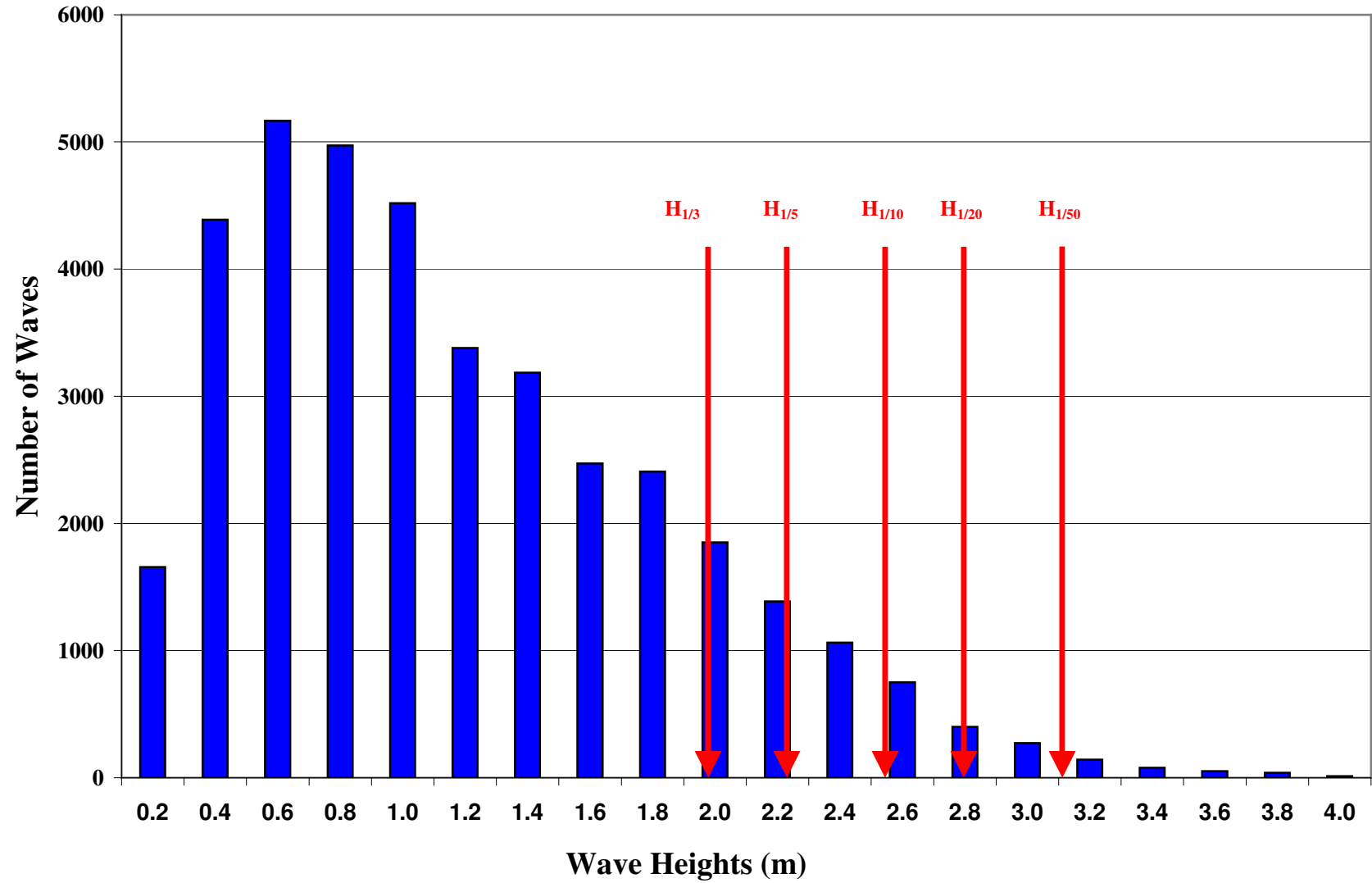equired to develop the grid used to compute wave transformation within the computation domain. It is critical to have a grid resolution fine enough to accurately model wave interaction with slope changes (shoaling, refraction) and barriers (reflection, diffraction). However, if the grid is too fine, computation time and effort can increase dramatically. The progression of grid development for this analysis is illustrated in figures 13.

Test model runs using the initial grid in figure 13-A showed the grid was too coarse for our modeling purposes. The inadequate resolution increased the influence of the boundary conditions producing asymmetric wave fields and unrealistically low wave climates in the harbor. Figure 13-B shows the improved grid. Sensitivity analysis of this grid proved it was adequate to model the harbor in the 2003 scenario. However, it was still too coarse for the 1938 scenario. As will be discussed later in this report, the 1938 layout of the harbor had more variations in the boundary conditions as well as more shallow regions requiring better resolution. Figure 13-C illustrates the much finer grid developed for the 1938 scenarios.
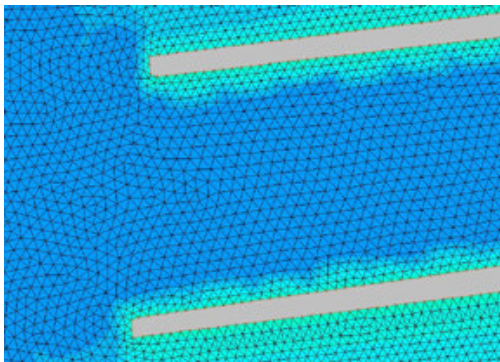
**A) Initial grid created
which was too coarse for
computations**
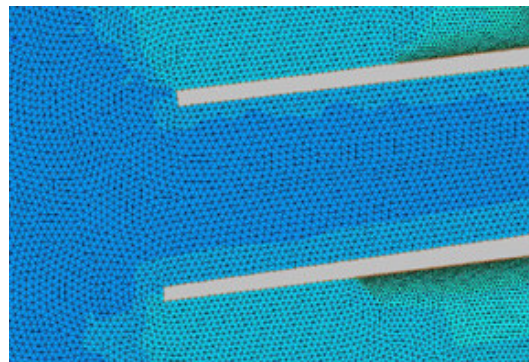
**B) Grid used in 2003
scenarios**
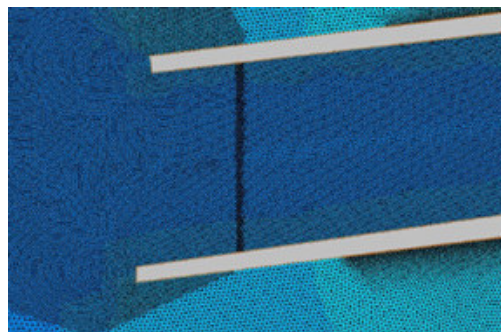
C) Grid used in 1938 scenario

Figure 13: Grid Layouts used in CGWAVE Modeling.

4.2.3   Reflection Coefficients (C_r)

A key boundary condition variable within the harbor is the reflection coefficient. Wave energy that enters a harbor must eventually dissipate. This primarily happens through 3 mechanisms: 1) diffraction 2) shoaling and 3) absorption. Diffraction is dependant on changes in geometry and the presence of obstacles, while shoaling is dependant on contour features. Absorption is dependant on the characteristics of the interior boundaries of the harbor and how much energy is absorbed at the boundaries. In modeling, a reflection coefficient is used to represent this mechanism. Reflection coefficients are dependent on the boundary slope, surface roughness, and porosity (CEM, 2004). Vertical wall structures, such as SSP, wood walls and concrete, have coefficients that approach unity, that is, almost all wave energy is reflected. At the other end of the spectrum, beach profiles typically have coefficients near zero and reflect almost no wave energy.

Initial design drawings of the harbor structures show they were stone filled timber crib structures. These structures consisted of two walls constructed of 12"x12" timbers layered on top of one another topped with a concrete cap. Stones were place between the walls to provide stability against wave energy and ice attack. As the structures began to fail, SSP was installed to encapsulate the old substructure. This was also capped with concrete. Figure 14 is a cross section of both the old and new structure designs.
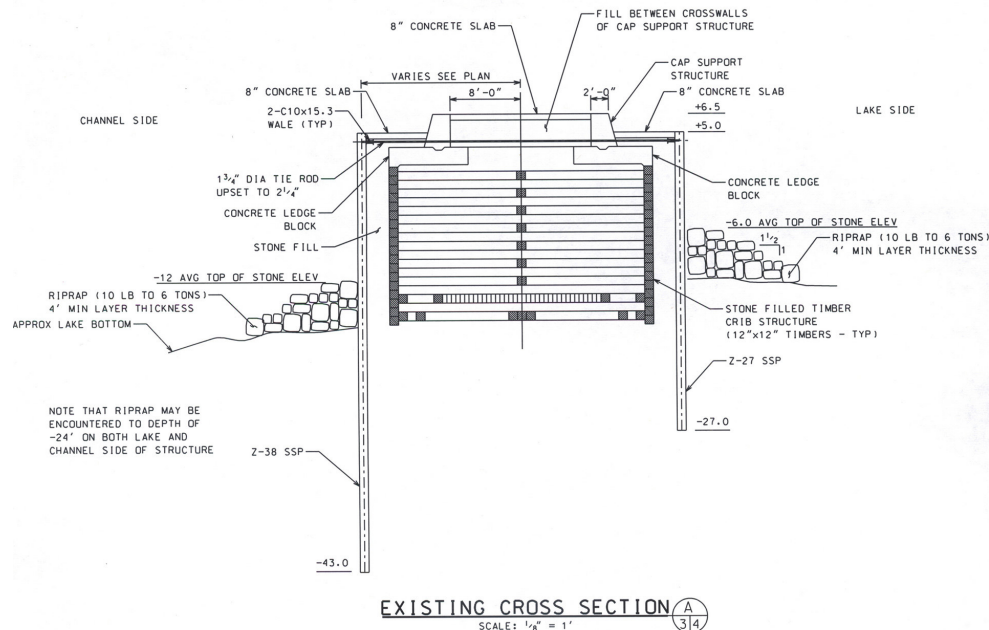

Figure 14: Existing Timber Crib Cross Section with new SSP Installation

Numerical modeling analyses required selection of three separate reflection coefficients, 1) for the SSP, 2) for the timber cribbing, 3) for the natural shoreline. Based on the current Coastal Engineering Manual (CEM, 2004) and consultation with the Engineering Research Development Center (ERDC), reflection coefficients for the natural shoreline were chosen to be zero (Cr = 0.0). This was mainly based on the fact that the natural shoreline was typically gently sloping sandy beach. In addition, reflection coefficients for both the SSP and timber cribbing were determined to be 0.9. After considerable investigation it was determined that SSP and timber wood cribbing would both represent typical rigid vertical bulkhead with an irregular facing surface. Figure 15 illustrates the irregular facing of the SSP. It was determined that this would not be more or less reflective than timber cribbing with voids between some members or imperfections in the wood.

Another important assumption was that the timber cribbing was structurally sound for the majority of its functional life prior to 1955. Table 1 seems to suggest that the harbor structures were relatively well maintained during its history. Stone exposure and dilapidation does not seem to represent a long temporal period in the life of the harbor.
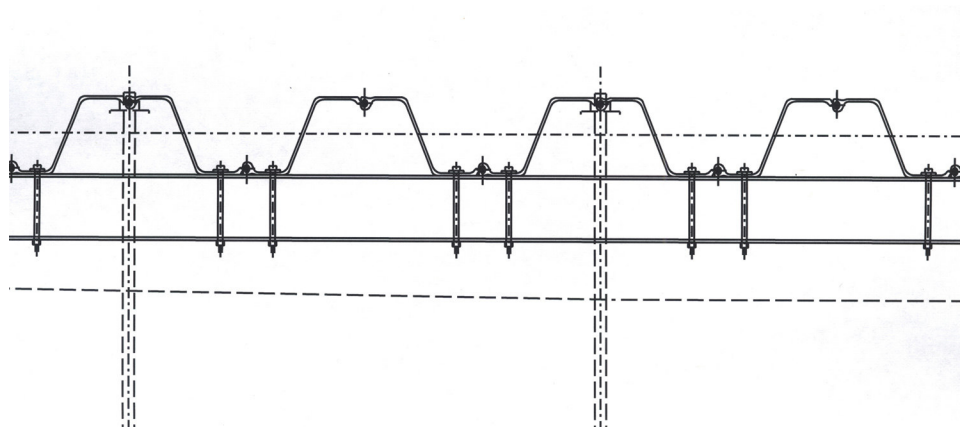
Figure 15: Irregularity in Facing Surface of SSP used at Grand Haven

5.0 Modeling Results

This section will cover the general results from the numerical modeling analysis. The two scenarios (1938 and 2003) will be discussed in further detail, wave conditions will be summarized for the model runs, and observations will be presented. This section will be elaborated on further in section 6.0.

5.1 Modeling Scenarios

Two separate modeling scenarios were chosen to investigate erosion at the study site. Since resources were limited in this analysis, domain creation for computations needed to be minimized while still obtaining sufficient results. Preliminary investigation of aerial

25

photography (see section 3.3) available indicated comparing the harbor layout in 1938 to the harbor layout in 2003 would best represent the changes in geometry seen at the harbor.

The main differences in the two scenarios can be seen in figure 3 on page 6. The harbor in 1938 had two areas along the north part of the channel that were unprotected, actively eroding shorelines. The study area seemed to be relatively stable in both the 1938 aerial photograph with the shoreline approximately 460 feet south of its present day position. In contrast, aerial photography after 1955 shows the north side of the harbor built up with shore protection extending along the north side of the channel to the study area. Also, the 2003 aerial photograph shows the full extent of the erosion at the study site.

5.2 Summary of Modeling Runs

As discussed in section 4.2.1, a Baird 1-D wave hindcast was used to determine design waves for use in the numerical modeling analysis. Based on the wave conditions, wave zones, and scenario layouts, a total of 50 model runs were accomplished for the 1938 and 2003 scenarios. Table 3 summarizes the wave input for the model runs.

Model Run	Scenario	Wave Condition	Wave Direction	Model Run	Scenario	Wave Condition	Wave Direction
1	2003	WC 1	224	26	1938	WC 1	224
2	2003	WC 1	242	27	1938	WC 1	242
3	2003	WC 1	260	28	1938	WC 1	260
4	2003	WC 1	278	29	1938	WC 1	278
5	2003	WC 1	296	30	1938	WC 1	296
6	2003	WC 2	224	31	1938	WC 2	224
7	2003	WC 2	242	32	1938	WC 2	242
8	2003	WC 2	260	33	1938	WC 2	260
9	2003	WC 2	278	34	1938	WC 2	278
10	2003	WC 2	296	35	1938	WC 2	296
11	2003	WC 3	224	36	1938	WC 3	224
12	2003	WC 3	242	37	1938	WC 3	242
13	2003	WC 3	260	38	1938	WC 3	260
14	2003	WC 3	278	39	1938	WC 3	278
15	2003	WC 3	296	40	1938	WC 3	296
16	2003	WC 4	224	41	1938	WC 4	224
17	2003	WC 4	242	42	1938	WC 4	242
18	2003	WC 4	260	43	1938	WC 4	260
19	2003	WC 4	278	44	1938	WC 4	278
20	2003	WC 4	296	45	1938	WC 4	296
21	2003	WC 5	224	46	1938	WC 5	224
22	2003	WC 5	242	47	1938	WC 5	242
23	2003	WC 5	260	48	1938	WC 5	260
24	2003	WC 5	278	49	1938	WC 5	278
25	2003	WC 5	296	50	1938	WC 5	296

Table 3: Summary of Model Runs

5.3 Modeling Observations

Results from the numerical modeling effort provided valuable insight on the physical processes affecting the harbor, wave climate, and the study area. By comparing the 2003 and 1938 scenarios on a general scale, the final analysis became more efficient. Modeling results for the harbor can be viewed in Appendix A.

A number of observations were made using the wave amplitude illustrations for the 1938 and 2003 scenarios in figure 16. Wave energy focusing and magnitude seems almost identical in the lakeside portion of the harbor for the two time periods. Wave patterns begin to deviate and wave energy intensifies within the channel around erosion area 1. For almost all model runs, the wave climate along the south side of the channel was elevated when compared to the north side. Wave propagation up the channel tended to be greatest for scenarios out of the southwest and west-northwest.

A) 1938 Scenario   B) 2003 Scenario
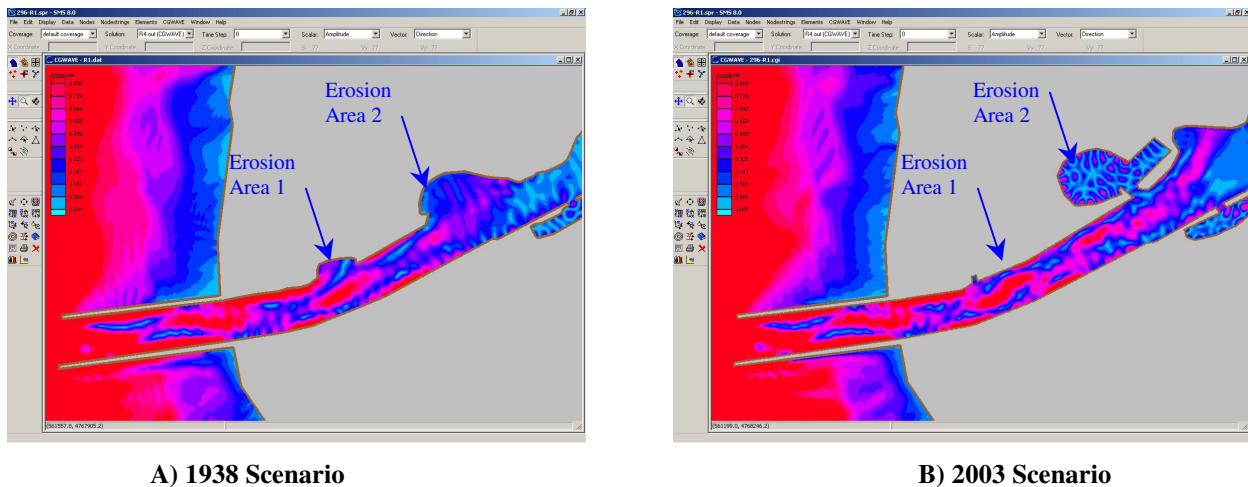
Figure 16: CGWAVE Modeling Results

Surprisingly, wave focusing at the study site was greatest for model runs with design wave heights equaling $H_{1/10}$ and $H_{1/20}$ from the southwest and for relatively smaller waves, $H_{1/3}$ and $H_{1/5}$, from the northwest. No wave energy seemed to reach the study site in the 1938 scenarios. It seemed that wave energy tended to be completely absorbed in both erosion areas 1 and 2. When these erosion areas were eliminated (present location of Coast Guard station and marina, respectively), as represented in the 2003 scenarios, wave energy started to reach the study site. In addition, a correlation could be seen between energy magnifications in front of the marina and wave focusing at the study site.

CGWAVE model results are available in Appendix A

6.0 Analysis and Results

In this section, the analysis procedure will be defined and results will be presented. Utilizing the data and modeling results shown in the previous sections, this investigation examines the extent of shore damage and erosion at Kitchel-Lindquist Dunes (study site) due to navigation improvements within Grand Haven Harbor. The analysis will include:

1. Recession rate calculation.
2. Reduction of modeling results.

6.1 Recession Rate Calculations

The aerial photography discussed in section 3.3 was used to calculate recession rates at the study site. Figure 17 illustrates the shoreline mapping accomplished from 1938 to 2003. It can be seen that minimal shoreline change occurred from 1938 to 1955. Furthermore, inspection of the 1955 aerial photograph shows that some sediment was removed from the area during construction of the marina making it hard to assess how much of the shoreline change, if any, during this temporal period was due to natural processes. It should also be noted that the 1997 shoreline delineation was omitted from the recession analysis because it was not possible to map the shoreline with sufficient accuracy.
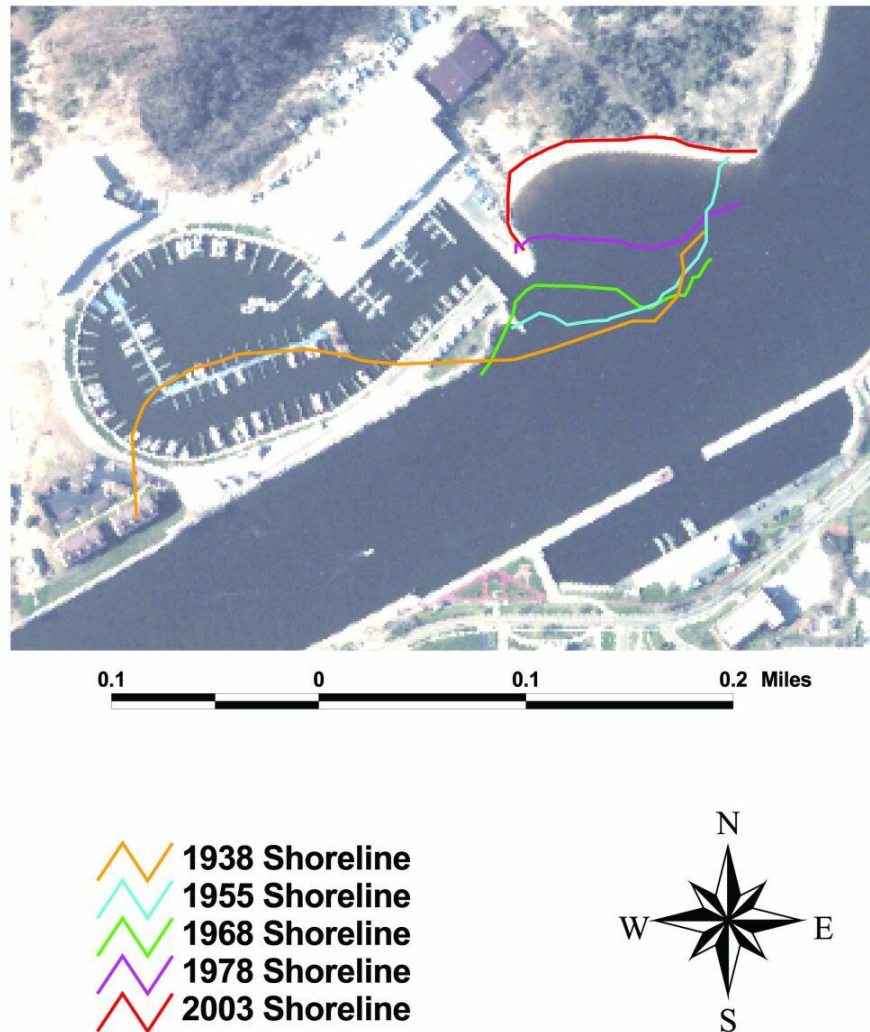
Figure 17: Shoreline Recession from 1938 to 2003

From 1955 to 2003 the shoreline has receded approximately 461 ft. Over this time period the recession rates have increased approximately 2.0 ft per year. The rate from 1955 to 1968 was 8.08 ft/yr. It increased to 10.17 ft/yr from 1969 to 1978 and remained constant at 10.17 ft/yr from 1978 to 2003.

Valuable insight into the effects SSP has on recession rates at the study site were obtained by comparing the shoreline recession from 1955 to 2003 with the percent changes in SSP coverage in the harbor. Figure 18 shows this comparison. The following assumptions were used in the development of figure 18.
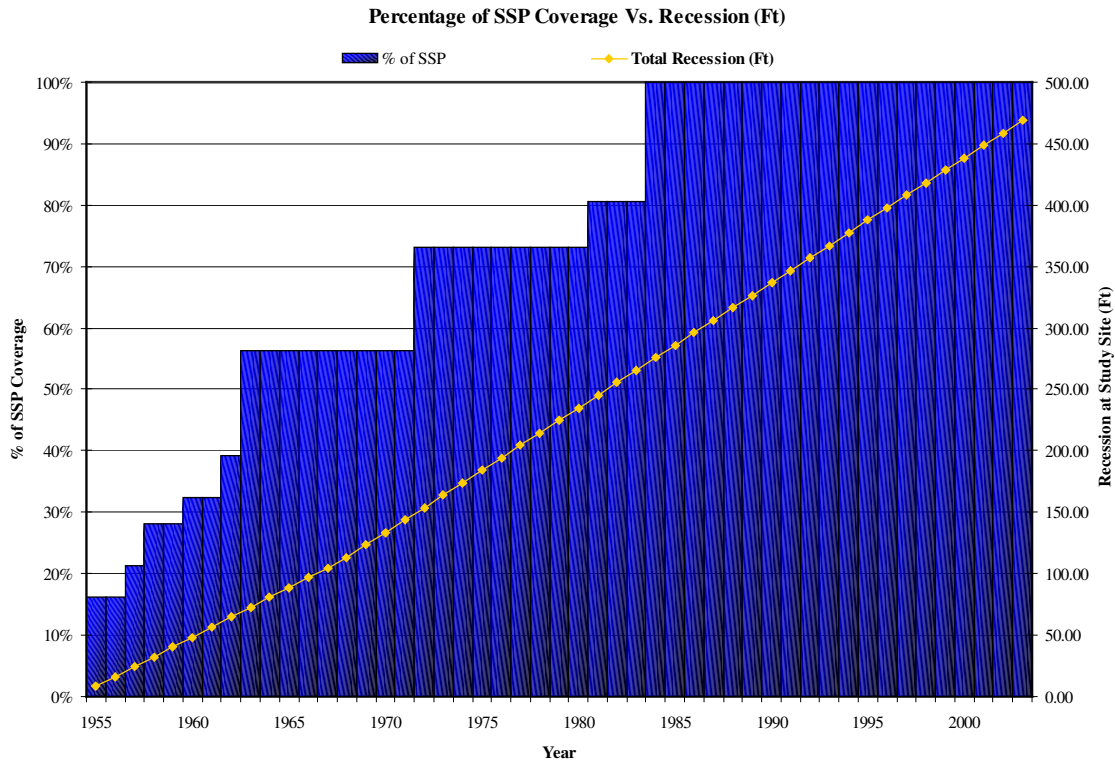
Figure 18: SSP Coverage vs. Recession

1.   Recession did not begin until 1955. This was supported by the 1938 and 1955 aerial photography analysis.
2.   Installation of SSP happened within one calendar year.
3.   Recession was constant between temporal periods defined by the aerial photography available.

It can be seen that the recession rate did not seem to fluctuate due to proliferation of SSP throughout the harbor. It would be expected that if the SSP were a direct contributor to the erosion problem at the study site recession rates would amplify as the SSP percentage rose. However, this was not the case. The increase of 2.0 ft/yr during this time frame is probably attributable to the repairs to the failing structures. It would be assumed that excessive voids in the timber cribbing had increased over the lifetime of the structure necessitating maintenance. These voids would have absorbed more wave energy than normal, potentially affecting the erosion at the study site. If the structures were never failing (i.e. the wood timbers remained structurally sound) then the normal recession rate for the study site would be expected to be 10.17 ft/yr with the 2003 harbor configuration.

Another interesting observation worth noting is that based on the geometry of the harbor, it would be expected that improvements to the south side of the channel at the bend (represented in figure 5 by the cyan and green lines) would have significant effects on wave focusing and erosion at the study site. This assumption was not collaborated this recession analysis nor in the CGWAVE analysis.

6.2 Reduction of Modeling Results

Observation arcs were created within the harbor (Figure 19) using the Surface Modeling System (SMS) to develop graphs illustrating wave amplitudes across the channel. Arc profiles 1-5 can be viewed in Appendix B. Analysis of these profiles did not provide any further information than provided by the model results in Appendix A.

Reduction of the modeling results required determination in the differences of wave energy propagation between the two modeling scenarios. Therefore, it was necessary to develop real-sea states within the harbor to quantify the wave energy that propagates up th e channel. To accomplish this, wave direction percentages were calculated from the five bearings modeled (Table 4) and used as weighting parameters for all five-wave conditions for both temporal periods. Using these results, Arcs A, B, and C were developed to show the wave energy differences between the 1938 and 2003 scenarios as a function design wave height. Appendix C shows all the energy profiles created.
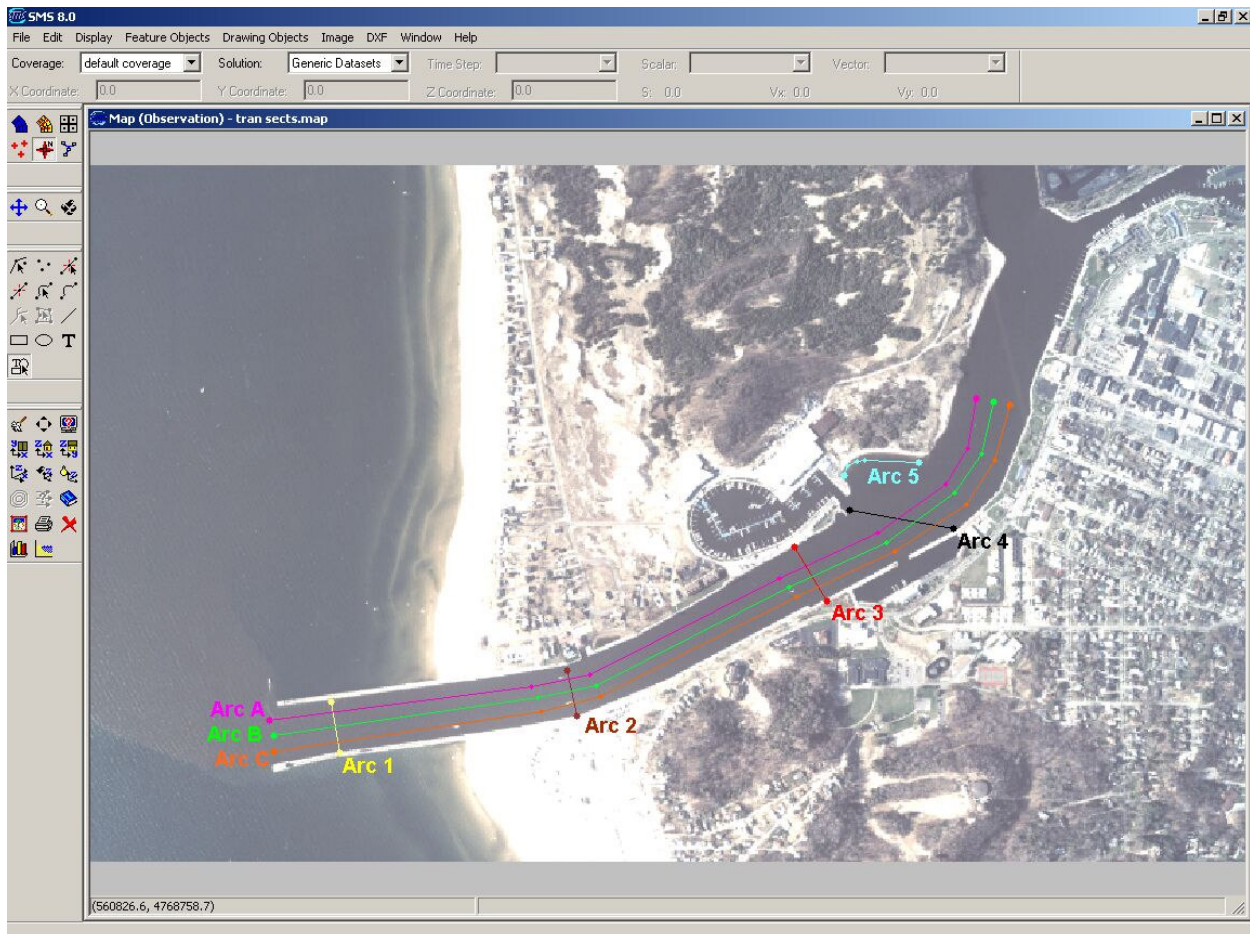
Figure 19: Observation Arcs

Wave Direction	Direction Frequency
224	24%
242	18%
260	16%
278	19%
296	23%

Table 4: Wave Direction Percentage

Analysis of the Arcs showed that there were seemingly no correlations in wave energy along Arc C and wave focusing at the study site. However, Arcs A and B showed an adequate link between wave energy focusing at the study site and wave energy increases due to improvements at erosion areas 1 and 2 shown in the 1938 scenario. Figures 20 and 21 illustrate this observation. It can be seen in these examples that the 2003 scenario showed a significant increase in wave energy at the marina and at the Coast Guard station. Inspection of the modeling results show that these fluctuations correlate to energy increases at the study site.
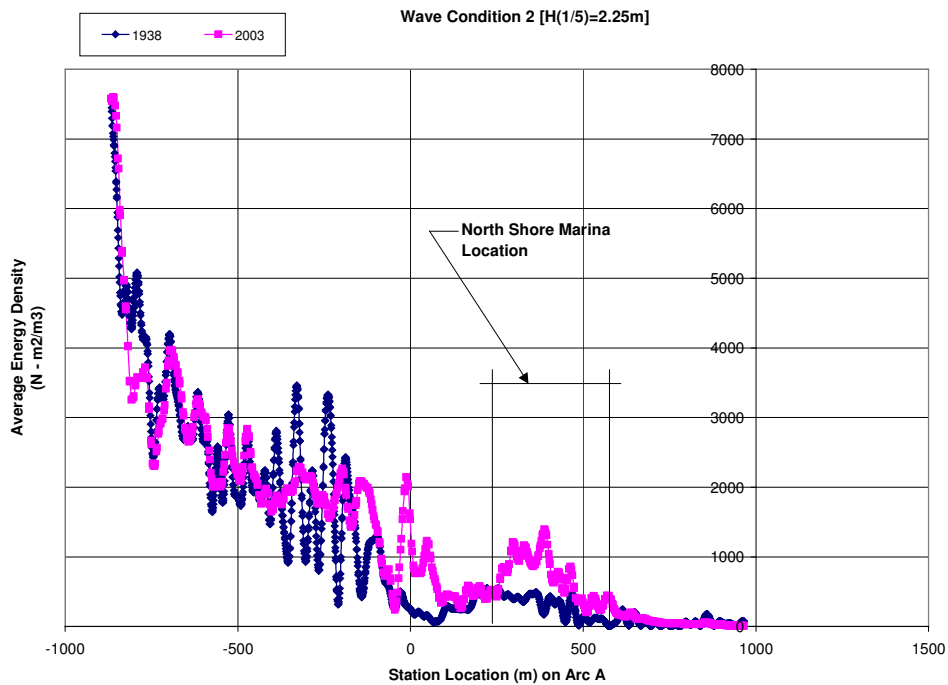
Figure 21: Energy Fluctuation-Arc A
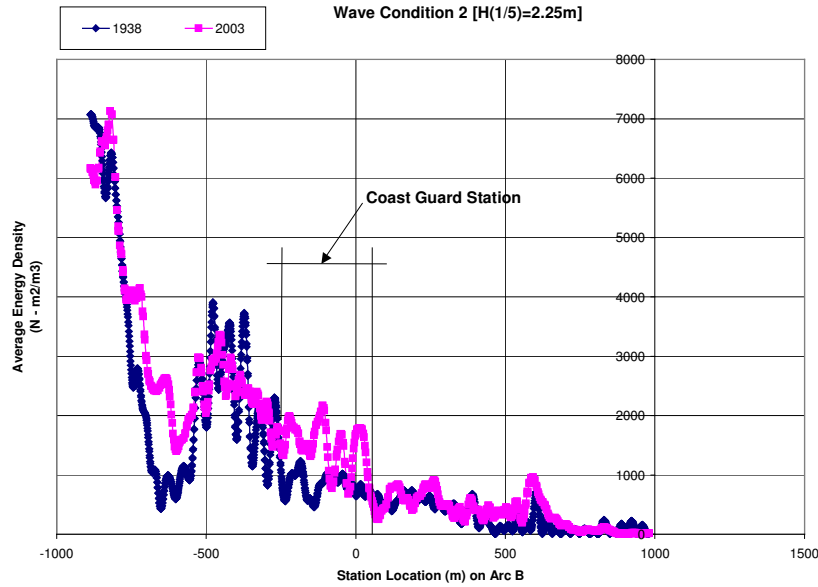
Figure 22: Energy Fluctuation-Arc B

Using the results from the wave energy profiles, the energy differences between the two temporal periods were quantified. For each wave condition (WC), wave direction and temporal period, energy was averaged across the profile in front of north marina (2003 scenario) and erosion area 2 (1938 Scenario) and in front of the Coast Guard station (2003 scenario) and erosion area 1 (1938 scenario). A real-sea state was achieved by weighting each WC based on the percentage within the five bearings modeled that the five WC occur.

Table 5 summarizes the wave energy calculation results for each location within the harbor. It can be seen that wave energy has increased considerably near the Coast Guard station and the north marina in the 2003 scenario.

Wave Energy ($^{N\text{-}m2}/_{m3}$)												
	Area Near North Shore Marina										**Total Energy by**	
Wave Condition	**$H_{1/3}$**		**$H_{1/5}$**		**$H_{1/10}$**		**$H_{1/20}$**		**$H_{1/50}$**		**Wave Dir.**	
Wave Direction	**1938**	**2003**	**1938**	**2003**	**1938**	**2003**	**1938**	**2003**	**1938**	**2003**	**1938**	**2003**
224	910	2684	1437	1983	1989	5170	2223	4772	1877	3333	1391	3113
242	1622	1920	2065	2727	2697	3762	2778	2795	1942	1327	2034	2482
260	1594	1906	1731	1619	2008	1232	2143	1038	1613	343	1748	1564
278	716	1626	486	1698	504	1060	747	1354	599	835	617	1491
296	1785	6947	1415	5788	581	1735	487	1312	397	1113	1306	5001
Total Energy By Wave Cond.	1312	3201	1411	2880	1513	2716	1630	2373	1263	1508	1397	2878

	Area Near Coast Guard Station										**Total Energy by**	
Wave Condition	**$H_{1/3}$**		**$H_{1/5}$**		**$H_{1/10}$**		**$H_{1/20}$**		**$H_{1/50}$**		**Wave Dir.**	
Wave Direction	**1938**	**2003**	**1938**	**2003**	**1938**	**2003**	**1938**	**2003**	**1938**	**2003**	**1938**	**2003**
224	5492	6121	6141	6493	10318	13703	11981	15784	12500	12041	7374	8600
242	4194	5001	5245	7103	8139	10401	8678	10093	8022	7998	5704	7041
260	1670	1735	1415	2417	3206	3752	3436	3756	3644	3781	2105	2526
278	1582	3332	1703	1593	594	503	535	476	600	798	1313	2026
296	4769	13848	9517	9268	3362	2978	1953	1601	943	1133	5381	9134
Total Energy By Wave Cond.	3738	6465	5157	5658	5340	6542	5538	6665	5358	5347	4620	6221

Table 5: Wave Energy Summary

The next step in this analysis is to correlate the energy increase at the Coast Guard station and north marina with the energy increase at the study site. In order to accomplish this a few assumptions were made:

1. Erosion area 2seen in the 1938 scenario is assumed to absorb all wave energy, meaning that no significant energy would pass this area. This is based on the results obtained from CGWAVE.
2. Based on inspection of the aerial photography, it is assumed that erosion at the study site did not start until 1955 when the marina was installed.
3. The study site is assumed to dissipate all the wave energy observed at the North Shore Marina location in the 2003 scenario.
4. In order to pinpoint the effects improvements at the Coast Guard station area are having at the study site, it is assumed that wave energy dissipation from the Coast Guard station area to the north marina location will be based on the energy difference in the 1938 scenario. This will eliminate any influence on wave energy that the marina improvements might have on wave energy. Based on this assumption, 70% of the wave energy was calculated to dissipate between the Coast Guard station and the north marina.
   - (4,620 – 1397) / 4,620 = 70%
5. Influences from structural improvements at the Coast Guard station location are assumed to begin in 1955.

Based on the data presented in Table 5, wave energy increased 1,601 N-M^2/M^3 in front of the Coast Guard Station and 1,481 N-M^2/M^3 near the north marina from 1938 to 2003. Assuming that 30% of the energy in front of the Coast Guard Station would translate down to the north

marina area results in approximately 480.00 N-M^2/M^3 of wave energy attributable to the improvements at the Coast Guard Station. Subtracting this amount of energy from the total wave energy increase at the north marina area results in about 1000.00 N-M^2/M^3 attributable to improvements at the north marina area. Based on the assumptions stated above, CGWAVE modeling conclusions indicate that potentially 32% (480.00/1481*100% = 32%) of the erosion at the study site can be attributed to Corps structure improvements.

7.0 Summary of Analysis Results and Conclusions

Through the use of state-of-the art numerical modeling, analysis of available aerial photography, and investigation of existing construction records, this study was able to determine the effects changes to the harbor area have had on erosion at Kitchel-Lindquist Dunes (study site).

- Analysis of the recession rates from 1955 to 2003 indicate that there was little correlation between the rate of recession and the increase of SSP encasement from 1955 to 2003. During this time the percentage of SSP coverage rose from 16% in 1955 to 100% in 1985. This represents a relatively large increase in SSP encasement. It would be anticipated that if recession at the study site were a result of these improvements to the harbor then the recession rate would increase significantly.

- Enhancements to the south side of the channel at the west end of the bend in the harbor channel showed no significant affect on recession rates at the study site. These improvements were accomplished in the early 1980's with no increase to the existing recession rate.

- CGWAVE results showed no evidence of wave energy reaching the study site prior to geometric changes in the 1950's. Since recession rates seemed pretty static from 1955 to present, it seems reasonable to conclude that SSP encasements have little effect on erosion at the study site.

- Analysis of aerial photography supports the conclusion based on CGWAVE results stated above. Erosion at the study site did not begin until around 1955, coinciding with two major alterations to the geometry of the harbor. The first alteration was the addition of revetment protection to the north portion of the channel near the present day Coast Guard Station. The second alteration was the installation of the marina on the north side of the channel.

- Quantification of wave energy along the axis of the channel resulted in a determination that federal improvements to the harbor could be responsible for up to 32% of the erosion at Kitchel-Lindquist Dunes. The remaining 68% is attributable to alterations made to harbor by other stakeholders.

References

American Association of State Highway and Transportation Officials (AASHTO) (1992). Standard Specifications of Highway Bridges, Washington, DC.

Assel, R.A. (1980) Great Lakes degree-day and temperature summaries and norms, 1897–1977. NOAA Data Report ERL GLERL-15, January 1980. Great Lakes Environmental Research Laboratory, Ann Arbor, MI.

Assel, R.A., F.H. Quinn, G.A. Leshkevich, and S.J. Bolsenga (1983) Great Lakes Ice Atlas. NOAA Atlas No.4.Great Lakes Environmental Research Laboratory, Ann Arbor, MI.

Baird, W.F., 1999, 1-D Wave Hindcast, Madison, WI

Baird, W.F., 2000, FEPS Development and Applications to the LMPDS Prototype Counties, Madison, WI

Battjes, J.A. (1982). "A case study of wave height variations due to currents in a tidal entrance." *Coast. Engrg.*, 6, 47-57.

Battjes, J.A., and Janssen, J.P.F.M. (1978). "Energy loss and set-up due to breaking of random waves." *Proc. 16th Coast. Engrg. Conf.*, ASCE, 569-587.

Berkhoff, J.C.W., Booij, N., and Radder, R.C. (1982). "Verification of numerical wave propagation   models for simple harmonic linear waves." *Coast. Engrg.*, 6, 255-279

Berkhoff, J.C.W. (1976). "Mathematical models for simple harmonic linear water waves wave refraction and diffraction." *Publ. 163*, Delft Hydraulics Laboratory.

Berkhoff, J.C.W. (1972). "Computation of combined refraction-diffraction." *Proc. 13th Intl. Coast.   Engrg. Conf.*, 741-790.

Chen, H.S. (1990) "Infinite Elements for water wave radiation and scattering." *Intl. J. Num. Meth. In Fluids*, 11,555-569.

Chen, H.S., and Houston, J.R. (1987). "Calculation of Water Level Oscillations in Harbors." *Instructional Report CERC-87-2*, Waterways Experiment Station, Vicksburg, Miss.

Dally, W.R., Dean, R.G., and Dalrymple, R.A. (1985) "Wave height variation across beaches of arbitrary profile." *J. Geophys. Res.*, 90, 1917-11927.

Dalrymple, R.A., Kirby, J.T., and Hwang, P.A. (1984). "Wave refraction due to areas of high energy dissipation." *J. Wtrway, Port, Coast., and Oc. Engrg.*, 110, 67-79.

Davis, J.E. (1992). "STWAVE theory and program documentation." Chapter 8 in Coastal Modeling System User's Manual, *Instructional Report CERC-91-1*, Supplement 1, Ed. M.A. Cialone, Waterways Experiment Station, Vicksburg, Miss.

Demirbilek, Z. (1994). "Comparison between REFDIFS and CERC Shoal Laboratory Study." *Unpubliashed Report*, Waterways Experiment Station, Vicksburg, Miss.

Demirbilek, Z., and Gaston, J.D. (1985). "Nonlinear wave loads on a vertical cylinder." *Oc.Engrg.*, 12, 375-385.

Demirbilek, Z. and Webster, W.C. (1992). "Application of the Green-Naghdi Theory of fluid sheets to shallow-water wave problems, Report 1: Model development, Report 2:User's manual and examples for GNWAVE" *Tech. Reports CERC-92-1 and CERC-92-13,* Waterways Experiment Station, Vicksburg, Miss.

Demirbilek, Z., XU, B., and Panchang, V. (1996a). "Uncertainties in the validation of harbor wave models." *Proc. 25th Intl. Coast. Engrg. Conf.*, 1256-1267.

Demirbilek, Z., Briggs, M., and Green, D. (1996b). "Wave-current interaction at Inlets." *Proc. 25th Intl. Coast. Engrg. Conf.*, 1219-1232.

De Girolamo, P., Kostense, J.K., and Dingemans, M.W. (1988). "Inclusion of wave breaking in a mild-slope model." Computer Modeling in Ocean Engineering, Balkema, Rotterdam, 221- 229.

Ebersole, B.A. (1985). "Refraction-diffraction model for linear water waves." *J. Wtrway., Port, Coast., and Oc. Engrg.*, 111,6.

Edil, T.B., Roblee, C.J., and Wortley, C.A. (1988) Design approach for piles subject to ice jacking. *Journal of Cold Regions Engineering*, Vol. 2, pp 65–85, June 1988.

Foltyn, E.P., and Tuthill, A.M. (1996) Design of ice booms. U.S. Army Cold Regions Research and Engineering Laboratory, April 1996. Technical Digest No. 96-1.

Hasselmann, K., Barnett, T.P., Bouws, E., Carlson, H., Cartwright, D.E., Enke, K., Ewing, J.A., Gienapp, H., Hasselmann, D.E., Kruseman, P., Meerburg, A., Muller, P., Olbers, D.J., Richter, K., Sell, W., and Walden, H. (1973). "Measurements of wind-wave growth and swell decay during the Joint North Sea Wave Project (JONSWAP)," *Deut. Hydrogr. Z., Suppl.* A, 8(12), 1-95.

Hubertz, et al. 1991. Wind Waves on the Great Lakes: A 32 Year Hindcast., Journal of Coastal Research, 7-4, p.945-967

Jones, N.L., and Richards, D.R. (1992). "Mesh generation for estuarine flow models." *J. Wtrway., Port, Coast., and Oc. Engrg.*, 118, 599-614.

Jonsson, I.G. (1990). "Wave-current interactions." Chapter 3 in *The Sea*, Vol.9, Part A, John Wiley & Sons, Inc., New York.

Kirby, J.T. (1986). " Higher order approximation in the parabolic equation method for water waves." *J. Geophys. Research*, 91, 933-952.

Kirby, J.T., and Dalrymple, R.A. (1984) "Verification of a parabolic equation for propagation of weakly-nonlinear waves." *Coast. Engrg.*, 8, 219-232.

Kirby, J.T. and Dalrymple, R.A. (1986). "An approximate model for nonlinear dispersion in monochromatic wave propagation models." *Coast. Engrg.*, 9, 545-561.

Kostense, J.K., Meijer, K.L., Dingemans, M.W., Mynett, A.E., and van den Bosch, P. (1986). "Wave energy dissipation in arbitrarily shaped harbours of variable depth." *Proc. 20th Intl. Conf. Coast. Engrg.*, 2002-2016

Li, B. (1994). "A generalized conjugate gradient model for the mild slope equation." *Coast. Engrg.*, 23, 215-225.

Liu, P.F.-F., and Tsay, T.K. (1984). " Refraction-diffraction model for weakly nonlinear water waves." *J. Fluid Mech.*, 141, 265-274.

Madsen, O.S. (1976). "Wave climate of the continental margin: Elements of its mathematical description." Marine Sediment Transport and Environmental Management, John Wiley, New York.

Mei, C.C. (1983). The Applied Dynamics of Ocean Surface Waves." John Wiley, New York.

Miche, M. (1951). "Le Pouvoir reflechissant des ouvrages maritimes exposes a l' action de la houle." *Annals des Ponts et Chaussess*, 121e Annee, 285-319 (translated by Lincoln and Chevron, Univ. Calif., Berkley, Wave Research Laboratory, Series 3, Issue 363, June 1954).

Panchang, V.G., Cushman-Roisin, B., and Pearce, B.R. (1988). "Combined refraction-diffraction of short waves for large coastal regions." *Coastal Engrg.*, 12, 133-156.

Panchang, V.G,, Ge, W., Cushman-Roisin, B., and Pearce, B.R. (1991). "Solution to the mild-slope wave problem by iteration." *Applied Ocean Research*, 13, 187-199.

Resio, D.T. (1987). "Shallow-water waves. I:theory." *J. Wtrway., Port, Coast., and Oc. Engrg.,*, ASCE, 264-281.

Resio, D.T. (1988a). "Shallow-water waves. II: data comparisons." *J. Wtrway., Port, Coast., and Oc. Engrg.*, ASCE, 114(1), 50-65.

Resio, D.T. (1988b). 'A steady-state wave model for coastal applications." *Proc. 21st Coast. Engrg. Conf.*, ASCE, 929-940.

Resio, D.T., and Perrie, W. (1989). "Implications of an f^4 equilibrium range for wind-generated waves." *J. Phys. Oceanography*, 19, 193-204.

Smith, J.M., Resio, D.T., and Vincent, C.L. (1997). "Current-induced breaking at an idealized inlet." *Proc. Coastal Dynamics '97*, ASCE, 993-1002.

Smith, S.J., and Smith J.M. (1998). "Modeling waves at Ponce de Leon Inlet, Florida." Submitted to *J. Wtrway., Port, Coast., and Oc. Engrg.,* ASCE.

U.S. Army Corps of Engineers, 2004, Coastal Engineering Manual, Coastal Engineering Research Center, Vicksburg, MS, 3 Volumes.

U.S. Army Corps of Engineers, 1984, Shore Protection Manual, Coastal Engineering Research Center, Vicksburg, MS, 3 Volumes.

U.S. Army Corps of Engineers, 1976, Section 111, Detailed Project Report, Detroit District, MI.

U.S. Army Corps of Engineers, 2004, Project Map Book (Grand Haven Harbor), Grand Haven Area Office (GHAO), MI.

U.S. Army Corps of Engineers, 2004, Regulatory Permitting Office, Grand Haven Area Office (GHAO), MI.

Wortley, C.A. (1985) Great Lakes small-craft harbor and structural design of ice conditions: An engineering manual. Sea Grant Report WIS-SG-84-426, University of Wisconsin, Madison.

Tsay, T.-K., and Liu, P.L.-F. (1983). "A finite element model for wave refraction and diffraction." *App. Oc. Res.*, 5, 30-37.

Vincent, C.L., and Briggs, M.J. (1989). "Refraction-diffraction of irregular waves over a mound." *J. Wtrway., Port, Coast and Oc. Engrg.*, 115, 269-284.

Xu, B., and Pachang, V.G. (1993) "Outgoing boundary conditions for elliptic water wave models." *Proc., The Royal Soc. Of Lon., Series A*, 441, 575-588.

Xu, B., Panchang, V.G., and Demirbilek, Z. (1996) "Exterior reflections in elliptic harbor wave models